PHYSICAL REVIEW A VOLUME 10, NUMBER 5 NOVEMBER 1974

# Effects of spectral cross relaxation and collisional dephasing on the absorption of light by organic-dye solutions

David W. Vahey
*Battelle Memorial Institute, Columbus, Ohio 43201*

Amnon Yariv
*California Institute of Technology, Pasadena, California 91109*
(Received 31 December 1973; revised manuscript received 22 April 1974)

The nonlinear absorption of intense laser light is used to obtain information about the times required for spectral cross relaxation ($T_3$) and collisional dephasing ($T_2$) in organic-dye solutions. The steady-state transmission experiment of Huff and DeShazer indicates that $T_2$ is in the range 0.1–1 psec for cryptocyanine-methanol, while $T_3$ is in the range 1–10 psec. For DDI-glycerin (1, 1′-diethyl-2, 2′-dicarbocyanine-iodide-glycerin), measurements of ultrashort-pulse transmission as a function of incident energy and optical polarization suggest a value $T_2 = 0.4 \pm 0.2$ psec for that system. These results are based on a new set of rate equations for absorption by inhomogeneously broadened organic-dye solutions. The equations display the effects of spectral cross relaxation and are not limited to light intensities less than those at which coherent interaction effects become important. For the case of ultrashort incident pulses, the equations are extended to account for excited-state absorption, the dependence of absorption on optical polarization, and the existence of a multiplicity of interacting excited states.

## I. INTRODUCTION

In many problems related to the interaction of light and matter, the material system is an ensemble of dipoles spread over a frequency band wider than the natural linewidth. Such systems are commonly described as inhomogeneously broadened. In gas and liquid absorbers, the resonance frequency of any single dipole migrates randomly across the band as it is acted upon by environmental forces. This process, called spectral cross relaxation, first received serious attention in connection with magnetic-resonance experiments in liquids.[1,2] For a system of liquid spins, cross relaxation is closely identified with the reorientational motion of the molecules to which the spins are attached. If this reorientation is sufficiently fast, the effects of local environmental inhomogeneities are averaged away. The absorbers interact with the radiation as would an ensemble of free spins.[3]

A similar situation arises in connection with absorption by optical dipoles in liquids. Here cross relaxation occurs as a result of configurational changes in the solvent environment about an absorbing solute molecule. If a system is exposed to monochromatic light of sufficiently low intensity, the cross-relaxation rate will greatly exceed the photon-absorption rate calculated from Fermi's golden rule. In this limit, the probability that an absorber will be excited during any one excursion into a condition of resonance with the wave is small, and the spectral distribution of unexcited molecules remains the thermal distribution. The situation is comparable to absorption by rapidly tumbling magnetic dipoles in the sense that the effective molecular environment seen by the radiation is a thermally averaged one.

This will not be the case at high incident flux, when the rate of photon absorption exceeds that of cross relaxation. In this limit unexcited molecules that diffuse into a condition of near resonance have a significant probability for absorption in the time before changes in the solvent environment once again cause a shift in their frequency. This is often what one intends to convey in describing a system as inhomogeneous. Experimentally, one observes that the absorption spectrum of the system is distorted by the high-intensity radiation.[4] A depression, or "hole," appears at the excitation wavelength as a result of the rapid, selective pumping of resonant molecules.

This phenomenon is well documented in the case of certain polymethine cyanine dyes used in passive $Q$ switching and mode locking of ruby and neodymium lasers.[5–7] The implication is that a correct description of the absorption of intense light by these dyes should take spectral cross-relaxation effects into account. To date, this has not been done. Most equations developed to describe the interaction of organic dyes with laser radiation[8–10] are limited to those low intensities and/or fast spectral cross-relaxation rates where hole burning is not important, and where the dye behaves as an homogeneously broadened system.

A further limitation of the conventionally employed rate equations is that they do not describe

absorption in the regime where coherent-interaction effects are important. These effects are associated, for example, with self-induced transparency[11] and photon echoes,[2,12] and they are significant when the photon-absorption rate and the collisional-dephasing rate $(1/T_2)$ become comparable. In view of the large $f$ numbers of organic dyes (on the order of unity) and the high intensities of available pulsed laser sources, the coherent-interaction regime appears to be experimentally accessible even for dye solutions at room temperature, where $T_2$ is less than a picosecond.

In Sec. II our objective is to develop a set of rate equations for organic dyes general enough to describe the effects of spectral cross relaxation and coherent interaction. In Sec. III we reduce the equations to forms that may be conveniently applied to the absorption experiments discussed in Sec. IV, where we use our results to obtain information about cross-relaxation and collisional-dephasing rates in several organic-dye systems: cryptocyanine-methanol and DDI-glycerin (1, 1′-diethyl-2, 2′-dicarbocyanine-iodide-glycerin).

## II. DERIVATION OF THE RATE EQUATIONS

Early papers on magnetic resonance in liquids have discussed the importance of spectral cross relaxation.[1,2] In particular, Hahn[2] was concerned with the degredation of spin echoes that resulted when the echoes were delayed by a time long compared to that required for the relaxation process. His analysis was based on the modified Bloch equations,

$$du/dt + [\omega_0 - \omega + \delta(t)]v = -u/T_2, \tag{1a}$$

$$dv/dt - [\omega_0 - \omega + \delta(t)]u + \omega_1 r = -v/T_2, \tag{1b}$$

$$dr/dt - \omega_1 v = -(r - r_0)/T_1. \tag{1c}$$

Here $\omega_0 - \omega$ is the detuning frequency at $t = 0$, and $\delta(t)$ describes the temporal detuning change that results from cross relaxation. These equations may be applied to the problem of optical absorption if we make the following identifications:

$$\vec{p}(x, t, \omega_0) = \vec{p}_0[-u(x, t, \omega_0)\cos(\omega t - kx) + v(x, t, \omega_0)\sin(\omega t - kx)] \tag{2}$$

is the dipole moment induced in an absorber by the polarized field $\vec{E}(x, t) = \hat{e}_x \mathcal{E}(x, t)\cos(\omega t - kx)$, where $\vec{p}_0$ is the dipole matrix element between initial and final states of the transition. Also in Eq. (1), $r(x, t, \omega_0)$ describes the population inversion induced by the wave, and

$$\omega_1 = (\vec{p}_0 \cdot \hat{e}_x)\mathcal{E}(x, t)/\hbar \tag{3}$$

is a frequency proportional to the field amplitude. As usual, $T_2$ and $T_1$ are phenomenological dephasing and deactivation time constants. The inclusion of damping terms in Eq. (1) means that $u$, $v$, and $r$ are to be interpreted as ensemble averages, rather than as quantities appropriate to individual dipoles.

Equation (1) would be directly applicable to the problem of light absorption by organic dyes but for the following complication: When dye molecules are optically excited, several deactivation mechanisms operate in addition to those commonly associated with $T_1$. For example, many dyes are known to cross into the triplet manifold following absorption.[5,9,10,13] Even when this does not occur, stimulated emission may still be frustrated by the decay of excited molecules from an interacting state $|a\rangle$ to some intermediate, nonresonant state $|c\rangle$. This could occur through vibrational deactivation[9,14,15] or through the realignment of solvent neighbors in response to changed dipole forces in the excited state.[16] As it now stands, Eq. (1c) does not account for this.

Another complication of importance is that we require a solution to Eqs. (1) in the regime where changes in $\delta(t)$ occur in a time comparable to or less than the time required for changes in $\omega_1(x, t)$. In this situation the equations are intractable, and an alternative approach to the problem is desired.

The basis for such an approach has been established by Karplus and Schwinger in their work on saturation in microwave spectroscopy.[17] One may consider the state vector $(u', v', r')$ of a single molecule that has had a strong collision at time $t_0$, but which has not collided since. The state vector is assumed to evolve according to the undamped Bloch equations, and so no longer represents an ensemble average. Following Karplus and Schwinger, these averages are obtained by summing the microscopic state vectors generated from all past times $t_0$, on the assumption that collisions occur randomly at a characteristic interval $T_2$. For the out-of-phase component of polarization, we write

$$v(x, t, \omega_0) = \int_{-\infty}^{t} \frac{dt_0}{T_2} e^{-(t-t_0)/T_2}[n_b(x, t_0+, \omega_0) \times v'(\omega_1, \omega_0 - \omega, t - t_0, -1) + n_a(x, t_0+, \omega_0) \times v'(\omega_1, \omega_0 - \omega, t - t_0, +1)], \tag{4}$$

where $v'(\omega_1, \omega_0 - \omega, t - t_0, \pm 1)$ is a solution of the undamped Bloch equation $d\vec{r}'/dt = \vec{\omega} \times \vec{r}'$ for the initial condition $\vec{r}'(t = t_0) = (0, 0, \pm 1)$. In general $\vec{r}' = (u', v', r')$ and $\vec{\omega} = (\omega_1(x, t), 0, \omega_0 - \omega + \delta(t))$. The coefficient $n_b(x, t_0+, \omega_0)$ in Eq. (4) describes the probability that the ground state $|b\rangle$ was left occupied by the collision at $t_0$, while $n_a(x, t_0+, \omega_0)$ is the probability of finding the system in the excited state $|a\rangle$ at $t_0+$. The relation $n_b + n_a = 1$ will gen-

erally not hold because of the decay of excited molecules from interacting state $|a\rangle$ to some intermediate, noninteracting state $|c\rangle$, as we have discussed. By taking $n_a = 0$, we will restrict consideration to systems for which rapid deactivation prevents stimulated emission from occurring.

Implicit in our use of undamped Bloch equations to determine $v'$ in Eq. (4) is the idea that $T_1$ decay from the intermediate state $|c\rangle$ does not occur between collisions. While there is no physical justification for such an assumption, our interest is in systems for which $T_2 \lesssim \frac{1}{10} T_1$. In this case little information would appear to be sacrificed by considering that collisions trigger $T_1$ decay with a probability $T_2/T_1$. This idea is mathematically expressed by the equation

$$n_b(x, t_0+, \omega_0) = n_b(x, t_0-, \omega_0) + (T_2/T_1) n_c(x, t_0-), \tag{5}$$

where $n_c(x, t_0-)$ is the fractional population of the intermediate state $|c\rangle$. The spectral variation of $n_c$ may be ignored, as we have done, if deactivation into the ground-state species absorbing at $\omega_0$ is equally likely for all excited molecules. If $g(\omega_0 - \bar{\omega}_0)$ is the normalized line-shape function of the inhomogeneous distribution, centered at $\bar{\omega}_0$, then

$$n_c(x, t) = 1 - \int_{-\infty}^{\infty} d\omega_0 g(\omega_0 - \bar{\omega}_0) n_b(x, t, \omega_0) \tag{6}$$

in the limit where stimulated emission is negligible.

Equation (5) is to be substituted for $n_b(x, t_0+, \omega_0)$ in Eq. (4) when we have extended it to account for spectral cross relaxation that may be collision induced. Let us consider a model for cross relaxation in which $\omega_0(t)$ is constant between dephasing collisions. At each collision there is a probability $T_2/T_3$ that $\omega_0(t)$ changes instantly to some new, uncorrelated value, so that we have

$$n_b(x, t_0+, \omega_0) = [1 - (T_2/T_3)] n_b(x, t_0-, \omega_0) + (T_2/T_3) \int_{-\infty}^{\infty} d\omega_0' \, g(\omega_0' - \bar{\omega}_0) n_b(x, t_0-, \omega_0') + (T_2/T_1) n_c(x, t_0-). \tag{7}$$

The first term on the right-hand side of this expression accounts for molecules that collide at time $t_0$ without cross relaxing, while the second term accounts for molecules that simultaneously collide and cross relax into $\omega_0$ from all frequencies $\omega_0'$. Since $T_3$ is the time required for configurational change of many nearest-neighbor solvent molecules, while $T_2$ is the characteristic interval between single solute-solvent collisions, the implicit assumption that $T_3 \geq T_2$ appears to be physically sound.

It is necessary to substitute Eq. (7) into (4) to provide a link between the instantaneous polarization $v(x, t, \omega_0)$ and the past history of the system. The integration of Eq. (4) appears to be quite complicated in view of the $t_0$ dependence of the population $n_b$ and the frequency $\omega_1$, on which $v'$ depends. However, we need be concerned with variations in $n_b$ and $\omega_1$ that take place over a few $T_2$. For organic dyes at room temperature, this amounts to about a picosecond. In the experiments to be described later, field amplitudes and sample populations vary but little in that time. To sufficient accuracy for present purposes, we may take $n_b(x, t_0, \omega_0) = n_b(x, t, \omega_0)$ and $\omega_1(x, t_0) = \omega_1(x, t)$ in evaluating Eq. (4). Since our model for spectral cross relaxation permits us to take $\delta(t) = 0$ in the undamped Bloch equations for $v'$, we have the analytic solution

$$v'(\omega_1, \omega_0 - \omega, t - t_0, -1) = (\omega_1/q) \sin q(t - t_0), \tag{8}$$

$$q^2 = \omega_1^2 + (\omega_0 - \omega)^2, \tag{9}$$

which leads to

$$v(x, t, \omega_0) = \frac{\omega_1(x, t) T_2}{1 + \omega_1^2(x, t) T_2^2 + (\omega_0 - \omega)^2 T_2^2} \left\{ n_b(x, t, \omega_0)[1 - (T_2/T_3)] + \int_{-\infty}^{\infty} d\omega_0' \, g(\omega_0' - \bar{\omega}_0) n_b(x, t, \omega_0')(T_2/T_3) + n_c(x, t)(T_2/T_1) \right\}. \tag{10}$$

The in-phase component of induced polarization, $u(x, t, \omega_0)$, may be derived in a manner parallel to that which we have used to obtain Eq. (10). The final result is $u(x, t, \omega_0) = -(\omega_0 - \omega) T_2 v(x, t, \omega_0)$.

The connection between the induced polarization and light absorption is established by the electromagnetic wave equation. Numerous papers on laser theory[18] and the theory of self-induced transparency[11,19] have shown how the wave equation may be rewritten in terms of two equations for the amplitude and phase of a nearly monochromatic signal that interacts with an inhomogeneous material system. In mks units the evolution of the wave amplitude $\mathcal{E}(x, t)$ is described by

$$\frac{\partial \mathcal{E}}{\partial x}+\frac{n_0}{c}\frac{\partial \mathcal{E}}{\partial t}=-\tfrac{1}{2}N_0\frac{\omega p_0}{\epsilon_0 n_0 c}\int_{-\infty}^{\infty}d\omega_0\, g(\omega_0-\bar{\omega}_0)v(x,t,\omega_0), \tag{11}$$

where $N_0$ is the absorber concentration and $n_0$ is the solvent refractive index. This expression shows no averaging over molecular orientations, as would be necessary for an ensemble of anisotropic absorbers. We are considering, for simplicity, the isotropic limit described by $\omega_1 \equiv (\vec{p}_0\cdot\hat{e}_x)\mathcal{E}(x,t)/\hbar = p_0\mathcal{E}(x,t)/\hbar$.

Equation (11) is conveniently rewritten as the photon-transport equation

$$\left(\frac{\partial}{\partial x}+\frac{n_0}{c}\frac{\partial}{\partial t}\right)F(x,t) = -N_0\sigma_h F(x,t)\langle n_{\text{eff}}(x,t,\omega_0)\mathcal{L}(F,\omega_0-\omega)\rangle_{\text{av}} \tag{12}$$

when we make the following identifications:

$$F(x,t)\equiv\tfrac{1}{2}\epsilon_0 c n_0 \mathcal{E}^2(x,t)/\hbar\omega \tag{13}$$

is the flux density of the wave;

$$\sigma_h = \omega p_0^2 T_2/\epsilon_0 c n_0 \hbar \tag{14}$$

is the homogeneous cross section with which molecules exactly on resonance with the wave interact;

$$\langle A(\omega_0)\rangle_{\text{av}} \equiv \int_{-\infty}^{\infty} A(\omega_0)g(\omega_0-\bar{\omega}_0)d\omega_0 \tag{15}$$

defines the average of any spectral function $A(\omega_0)$ over the inhomogeneous linewidth;

$$n_{\text{eff}}(x,t,\omega_0) = n_b(x,t,\omega_0)[1-(T_2/T_3)] + \langle n_b(x,t,\omega_0)\rangle_{\text{av}}(T_2/T_3) \tag{16}$$

is an effective ground-state population; and

$$\mathcal{L}(F,\omega_0-\omega) = [1+2F\sigma_h T_2+(\omega_0-\omega)^2T_2^2]^{-1} \tag{17}$$

is a modified Lorentzian function. In Eq. (16) we have omitted a contribution $n_c(x,t)(T_2/T_1)$ from the right-hand side because of the assumed smallness of the ratio $T_2/T_1$. We may note that when $n_b(x,t,\omega_0)=\langle n_b(x,t,\omega_0)\rangle_{\text{av}}$ in Eq. (16), and when $2F\sigma_h T_2$ may be neglected in Eq. (17), the photon-transport Eq. (12) reduces to that conventionally used to describe light absorption by organic dyes.

A companion rate equation for the population $n_b(x,t,\omega_0)$ may be obtained from an integral expression parallel to that of Eq. (4):

$$n_b(x,t,\omega_0) = \int_{-\infty}^{t}\frac{dt_0}{T_2}e^{-(t-t_0)/T_2}\{n_b(x,t_0+,\omega_0)\tfrac{1}{2}[1-r'(\omega_1,\omega_0-\omega,t-t_0,-1)]\}. \tag{18}$$

The integral over $t_0$ is evaluated to sufficient precision if we take $\omega_1(x,t_0)=\omega_1(x,t)$ as before, while employing the Taylor-series approximation

$$n_b(x,t_0,\omega_0)\cong n_b(x,t,\omega_0)-(t-t_0)\frac{\partial}{\partial t}n_b(x,t,\omega_0)$$

in Eq. (7) for $n_b(x,t_0+,\omega_0)$. The quantity

$$\tfrac{1}{2}[1-r'(\omega_1,\omega_0-\omega,t-t_0,-1)] = \tfrac{1}{2}[1+q^{-2}(\omega_0-\omega)^2+q^{-2}\omega_1^2\cos q(t-t_0)] \tag{19}$$

describes the evolution of ground-state population in the interval $t-t_0$. In the first-order differential equation that is obtained by evaluating the $t_0$ integral of Eq. (18), not all terms in the resulting expression represent an intuitive extension of the conventional population rate equation. The added terms will have a small effect in the problems to which we will apply the theory. If we omit these terms for purposes of clarity, the resulting population rate equation has the form

$$\frac{\partial}{\partial t}n_b(x,t,\omega_0) = -\sigma_h F(x,t)n_{\text{eff}}(x,t,\omega_0)\mathcal{L}(F,\omega_0-\omega) -[n_b(x,t,\omega_0)-\langle n_b(x,t,\omega_0)\rangle_{\text{av}}]/T_3 +n_c(x,t)/T_1. \tag{20}$$

This equation and the photon-transport Eq. (12) constitute the basic theoretical results of this paper.

## III. ANALYSIS OF THE RATE EQUATIONS

Nearly all experiments that have been concerned with the absorption of intense light by organic-dye solutions make use of laser pulses that last on the order of $10^{-8}$ sec (giant pulses) or $10^{-11}$ sec (ultrashort pulses). A class of experimentally interesting absorbers is that for which $T_1$ and $T_3$ relaxation times are long or short compared to either of these two extremes. In describing such absorbers, the equations obtained in Sec. II may be simplified as follows: If pulse duration is long compared to $T_1$ and $T_3$, then $\partial/\partial t\to 0$ in the rate equations. This is the steady-state limit. If pulse duration is much less than $T_1$ and $T_3$, then $T_1, T_3\to\infty$ in the equations. We will refer to this as the short-pulse limit.

### A. Steady-state rate equations

As discussed in the Introduction, one possible effect of excitation by intense, monochromatic light is the creation of a spectral hole in a sample's absorption band. For steady-state conditions, this idea may be tested using the time-independent form of Eq. (20). We assume a ground-state population distribution

$$n(x, \omega_0) = n_2 - (n_2 - n_1)\{1 + [2(\omega_0 - \omega)/\delta\omega]^2\}^{-1}, \tag{21}$$

where $n_1 = n(x, \omega)$ is the population of unexcited molecules at the center of a proposed spectral hole of width $\delta\omega$, and $n_2 = n(x, \infty)$ is the population far outside the hole. [Note that we have suppressed the subscript $b$ from the ground-state population $n_b(x, \omega_0)$.] As long as the width of the postulated hole is small in comparison to the width of the inhomogeneous distribution $g(\omega_0 - \bar{\omega}_0)$, the Lorentzian term in Eq. (21) may be considered to have $\delta$-function character for purposes of evaluating $\langle\ \rangle_{av}$ expressions. We have, for example,

$$\langle n(x, \omega_0)\rangle_{av} = n_2 - \tfrac{1}{2}\pi(n_2 - n_1)g(\omega - \bar{\omega}_0)\delta\omega. \tag{22}$$

Substituting Eqs. (21) and (22) into Eq. (20), with $\partial/\partial t = 0$, we obtain an algebraic relation connecting unknowns $n_1$, $n_2$, and $\delta\omega$. Two independent equations result from setting $\omega_0$ separately equal to $\omega$ and $\infty$ in this relation. A third equation results from performing the operation $\langle\ \rangle_{av}$ on each term of Eq. (20). We find

$$0 = -\sigma_h F(x, t)\langle n_{eff}(x, t, \omega_0)\mathfrak{L}(F, \omega_0 - \omega)\rangle_{av} + (1 - \langle n\rangle_{av})/T_1. \tag{23}$$

The term $\langle n_{eff}(x, t, \omega_0)\mathfrak{L}(F, \omega_0 - \omega)\rangle_{av}$ is to be evaluated from the defining relations, Eqs. (16) and (17), with the help of Eq. (21). Again, $g(\omega_0 - \bar{\omega}_0)$ is to be assumed spectrally broad in comparison to $\delta\omega$ and $1/T_2$. The three equations in unknowns $n_1$, $n_2$, and $\delta\omega$, determined as we have just outlined, have the solutions

$$n_1 = \frac{1 + F\sigma_h T_2 + F\sigma T_2 Q}{1 + F\sigma_h(T_2 + T_3) + F\sigma(T_1 + T_2 - T_3)Q}, \tag{24}$$

$$n_2 = \frac{1 + F\sigma_h(T_2 + T_3) + F\sigma T_2 Q}{1 + F\sigma_h(T_2 + T_3) + F\sigma(T_1 + T_2 - T_3)Q}, \tag{25}$$

$$\delta\omega = 2Q/T_2, \tag{26}$$

where

$$Q = [1 + F\sigma_h(T_2 + T_3)]^{1/2}, \tag{27}$$

and

$$\sigma = \sigma_h \pi g(\omega - \bar{\omega}_0)/T_2 \tag{28}$$

is the inhomogeneous absorption cross section, determined from low-intensity wave attenuation in accord with Beer's law.

These results may be used in conjunction with the photon-transport Eq. (12) to obtain a differential equation for the steady-state flux density $F(x)$. In view of Eq. (23), we have

$$dF/dx = -N_0(1 - \langle n\rangle_{av})/T_1. \tag{29}$$

Using the results of Eqs. (24) through (26) to express $\langle n\rangle_{av}$ in terms of $F(x)$, we arrive at the following expression for the intensity-dependent absorption coefficient:

$$\alpha(F) \equiv -\frac{1}{F}\frac{dF}{dx} = \frac{N_0\sigma}{Q + F\sigma(T_1 + T_2 - T_3)}. \tag{30}$$

In order that our theory may better describe real organic dyes, let us now allow for the possibility that molecules excited to state $|c\rangle$ absorb homogeneously with a cross section $\sigma'$. The modified absorption coefficient is $\alpha(F) = \alpha(F)|_{\sigma'=0} + N_0\sigma'(1 - \langle n\rangle_{av})$, or

$$\alpha(F) \equiv -\frac{1}{F}\frac{dF}{dx} = N_0\sigma\frac{1 + F\sigma' T_1}{Q + F\sigma(T_1 + T_2 - T_3)}. \tag{31}$$

Wave transmission through a thickness $x$ of sample is obtained by integrating this equation, with the result

$$G(Q(x)) = G(Q(0)) - N_0\sigma x, \tag{32a}$$

$$G(Q) = \ln[(Q - 1)/(Q + 1)] + 2(\delta - 1)^{1/2}\tan^{-1}[Q/(\delta - 1)^{1/2}] + (\gamma)\ln[1 + (Q^2 - 1)/\delta], \tag{32b}$$

$$\delta = \sigma_h(T_2 + T_3)/\sigma' T_1, \tag{32c}$$

$$\gamma = \sigma(T_1 + T_2 - T_3)/\sigma' T_1. \tag{32d}$$

For a given input flux density $F(0)$, the steady-state transmission is

$$\frac{F(x)}{F(0)} = \frac{Q^2(x) - 1}{Q^2(0) - 1}.$$

It is this quantity that is measured in experimental studies of giant-pulse absorption by organic dyes.[9,10] Usually $F(0)$ is taken to be the flux density at the peak of the incident pulse, and $F(x)$ is the peak transmitted flux density.

The above derivation is based on an assumption that $\delta\omega \ll \Delta\omega$, where $\Delta\omega \cong 1/g(0)$ is introduced to describe the width of the inhomogeneous distribution. In view of Eq. (26), this condition is equivalent to $Q \ll \frac{1}{2}\Delta\omega T_2$ and is always violated at sufficiently high light intensities. In this limit, an analytic expression for the absorption coefficient is not available. One must appeal directly to the rate equations (12) and (20) to characterize wave attenuation.

In Sec. IV we will see that Eq. (32) is useful in describing the absorption of giant ruby-laser pulses in cryptocyanine-methanol up to intensities of $\sim 10^9$ W/cm$^2$.

### B. Short-pulse rate equations

We now turn our attention to the simplified forms of the rate equations that result when terms de-

scribing $T_1$ and $T_3$ relaxation processes may be neglected. In a frame of reference moving with an incident pulse,

$$\frac{\partial}{\partial x}F(x,t) = -N_0\sigma_h F(x,t)\langle n(x,t,\omega_0)\mathfrak{L}(F,\omega_0-\omega)\rangle_{\rm av}\ , \tag{33}$$

$$\frac{\partial}{\partial t}n(x,t,\omega_0) = -\sigma_h F(x,t)n(x,t,\omega_0)\mathfrak{L}(F,\omega_0-\omega)\ . \tag{34}$$

These equations may be uncoupled if $2F\sigma_h T_2 \ll 1$, so that $\mathfrak{L}(F,\omega_0-\omega)\cong\mathfrak{L}(0,\omega_0-\omega)$. It is this limit that we will consider. Equation (34) has the integral

$$n(x,t,\omega_0) = \exp[-W(x,t)\mathfrak{L}(0,\omega_0-\omega)], \tag{35}$$

$$W(x,t) \equiv \int_{-\infty}^{t} F(x,t')\sigma_h\,dt'\ . \tag{36}$$

Substitution of this result into Eq. (33) and subsequent integration over time yield

$$\partial W/\partial x = -N_0\sigma_h f(W), \tag{37a}$$

$$f(W) = \langle 1-\exp[-W(x,t)\mathfrak{L}(0,\omega_0-\omega)]\rangle_{\rm av}\ . \tag{37b}$$

Usually, one is interested in measuring the fraction of incident pulse energy transmitted by an absorber of thickness $x$ and concentration $N_0$. This is given by the ratio $W(x,\infty)/W(0,\infty)$, which may be determined by numerical integration of Eq. (37). In practice, however, the equation is of limited use in describing real absorbing systems. Some of the complexities of real systems have been suggested in previous discussion, yet were not considered in developing the fundamental rate equations (12) and (20). In order that our theory may better describe experimental data to be presented in Sec. IV, we now consider how Eq. (37) may be generalized to account for excited-state absorption, the dependence of absorption on molecular anisotropy, and the existence of a multiplicity of interacting excited states, $\{|a_i\rangle\}$.

(i) Excited-state absorption has been discussed in connection with steady-state solutions of the rate equations. We again assume that molecules in state $|c\rangle$ can absorb homogeneously with a cross section $\sigma'$, so that a term $-N_0\sigma' F(1-\langle n\rangle_{\rm av})$ is to be added to the right-hand side of Eq. (33). Now the insertion of Eq. (35) and subsequent integration over time yield

$$\partial W/\partial x = -N_0\sigma_h f(W) - N_0\sigma'\int_0^W f(W')\,dW'\ . \tag{38}$$

(ii) Properly accounting for molecular anisotropy leads to an energy attenuation equation that depends on optical polarization. For large molecules $\vec{p}_0 = \langle a|\hat{p}|b\rangle$ is well defined with respect to a coordinate frame attached to the molecule. The fact that solute absorbers are usually randomly oriented means that not all molecules can interact equally with incident radiation.

Consider a system where $\vec{p}_0$ lies in the direction of a long molecular axis. In the laboratory coordinate frame

$$\vec{p}_0 = |\vec{p}_0|(\sin\theta\cos\varphi, \sin\theta\sin\varphi, \cos\theta), \tag{39}$$

where zenith angle $\theta$ and azimuthal angle $\varphi$ define the molecular orientation. Transitions are excited by a field $\mathcal{E}_0(0,\epsilon_1,\epsilon_2)e^{-i\omega t}$, where $\hat{\epsilon} = (0,\epsilon_1,\epsilon_2)$ is a complex unit vector that describes the ellipticity of the polarized incoming wave. In particular $\hat{\epsilon} = (0,0,1)$ and $\hat{\epsilon} = (0,i,1)/\sqrt{2}$ designate linearly and circularly polarized waves, respectively. Using the relation $\sigma_h \propto |\vec{p}_0\cdot\hat{\epsilon}|^2$, we find

$$(\sigma_h)_{\rm eff} = \sigma_h|\Omega|^2, \tag{40}$$

where $\Omega = \cos\theta$ for linearly polarized light and $\Omega = (\cos\theta + i\sin\theta\sin\varphi)/\sqrt{2}$ for circularly polarized light.

To account for this dependence of absorption on molecular orientation, $\sigma_h$ must be replaced by $\sigma_h|\Omega|^2$ where it appears in Eqs. (33) and (34). In the photon-transport Eq. (33), all molecular orientations must be averaged. Thus,

$$\frac{\partial}{\partial x}F(x,t) = -N_0\sigma_h F(x,t)\langle|\Omega|^2 n(x,t,\omega_0)\mathfrak{L}(0,\omega_0-\omega)\rangle_{\rm av}\ , \tag{41}$$

where now

$$\langle|\Omega|^2 n(x,t,\omega_0)\mathfrak{L}(0,\omega_0-\omega)\rangle_{\rm av} = \int_{\theta,\varphi}\frac{1}{4\pi}\sin\theta\,d\theta\,d\varphi\,|\Omega|^2 \times\int_{-\infty}^{\infty}d\omega_0\,g(\omega_0-\bar{\omega}_0)n(x,t,\omega_0)\mathfrak{L}(0,\omega_0-\omega)\ . \tag{42}$$

The generalization of Eq. (37) is found to be

$$\frac{\partial}{\partial x}W(x,t,\hat{\epsilon}) = -N_0\sigma_h f(W), \tag{43a}$$

$$f(W) = \langle 1-\exp[-W|\Omega|^2\mathfrak{L}(0,\omega_0-\omega)]\rangle_{\rm av}\ . \tag{43b}$$

The notation $W(x,t,\hat{\epsilon})$ is used to show the dependence of pulse transmission on optical polarization. It is important to note that these results apply only if changes in molecular orientation do not occur over the duration of the pulse. Otherwise, relaxation terms would have to be introduced to describe random molecular migration between different orientations.

(iii) Finally, we consider how the energy-attenuation equations [either Eqs. (37), (38), or (43)] are

to be modified when there is a multiplicity of excited states $|a\rangle, |a_1\rangle, |a_2\rangle, \ldots$ that have a significant Franck-Condon overlap with the ground state. If the strongest transition is centered at $\bar{\omega}_0$ and the $i$th secondary transition is centered at $\bar{\omega}_0 + \Delta_i$, we must make the substitution

$$\mathcal{L}(0, \omega_0 - \omega) \to \mathcal{L}(0, \omega_0 - \omega) + \sum_i k_i^2 \mathcal{L}(0, \omega_0 + \Delta_i - \omega) \tag{44}$$

in Eqs. (33) and (34), where $k_i^2$ is the relative Franck-Condon factor of the $i$th transition.

The absorption spectrum of the molecule described by this multiplicity of Lorentzians is

$$\sigma(\omega - \bar{\omega}_0) = \sigma_h \frac{\pi}{T_2}\left(g(\omega - \bar{\omega}_0) + \sum_i k_i^2 g(\omega - \bar{\omega}_0 - \Delta_i)\right), \tag{45}$$

so that all $\{k_i\}$, $\{\Delta_i\}$, and the ratio $\sigma_h/T_2$ may be estimated by matching Eq. (45) to an experimental spectrum. Generally the inhomogeneous distribution function is chosen to be the Gaussian,

$$g(\omega_0 - \bar{\omega}_0) = \frac{(2/\pi)^{1/2}}{\Delta\omega} \exp\left(-2\frac{(\omega_0 - \bar{\omega}_0)^2}{\Delta\omega^2}\right). \tag{46}$$

## IV. MEASUREMENTS OF SPECTRAL CROSS RELAXATION AND COLLISIONAL DEPHASING IN ORGANIC-DYE SOLUTIONS

Since the first use of the polymethine dye cryptocyanine to $Q$ switch the ruby laser,[20] there has been an active experimental interest in the response of this molecule, and others like it, to the intense radiation it helps to make possible. Investigations on organic dyes have been principally concerned with spectral hole burning,[5,6,7,21] nonlinear absorption of intense light in violation of Beer's law,[9,10] and transient recovery of absorption following ultrashort-pulse excitation.[22]

The theory developed in this paper provides a means to describe these experiments in the case of inhomogeneous systems, where the rate of cross relaxation between different homogeneous components may strongly influence the data. We believe that our conclusions justify a reexamination of previously published experiments on cryptocyanine (1, 1′-diethyl-4, 4′-carbocyanine iodide).[5,6,9,10] In Sec. IV A we will consider the nonlinear transmission behavior of the molecule as determined by Huff and DeShazer.[9] Then we will present a complementary set of observations of our own on another polymethine $Q$-switch dye, DDI (1, 1′-diethyl-2, 2′-dicarbocyanine iodide). The results will show that information about the rates of collisional dephasing and cross relaxation in liquids may be obtained from simple experiments employing intense light.

### A. Giant-pulse transmission in cryptocyanine-methanol

#### *1. Experimental results of Huff and DeShazer*

Figure 1 shows the intensity dependence of transmission for a solution of cryptocyanine-methanol. In these data of Huff and DeShazer (HDS),[9] giant ruby-laser pulses of varying peak intensity are passed through a sample of minimum transmission 20%. Significant violation of Beer's law begins in the range $10^6$–$10^7$ W/cm$^2$. The transmission of the solution increases to about 70% at $10^8$ W/cm$^2$ and then begins to decrease.

To explain this behavior, Huff and DeShazer propose the molecular model of Fig. 2. Based on the

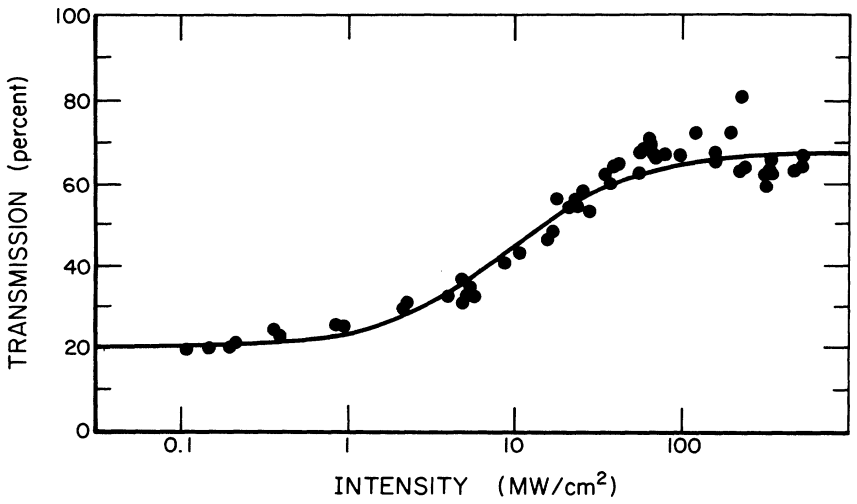


FIG. 1. Transmission-vs-intensity behavior of cryptocyanine-methanol, after Huff and DeShazer (Ref. 9).

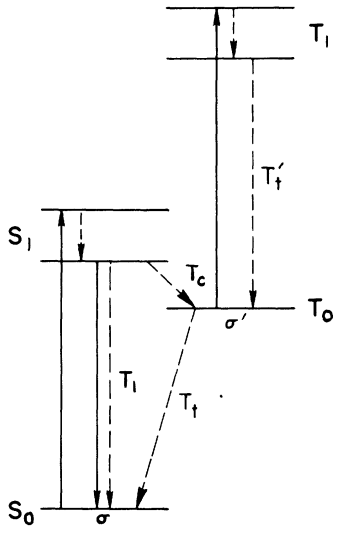


FIG. 2. Molecular model proposed by Huff and DeShazer (Ref. 9) to explain the data of Fig. 1. $S$ and $T$ refer to singlet and triplet states, respectively. Solid (dashed) lines describe radiative (nonradiative) transitions. Cross sections and relaxation times are defined in the text. Unlabeled nonradiative transitions are assumed to occur infinitely fast.

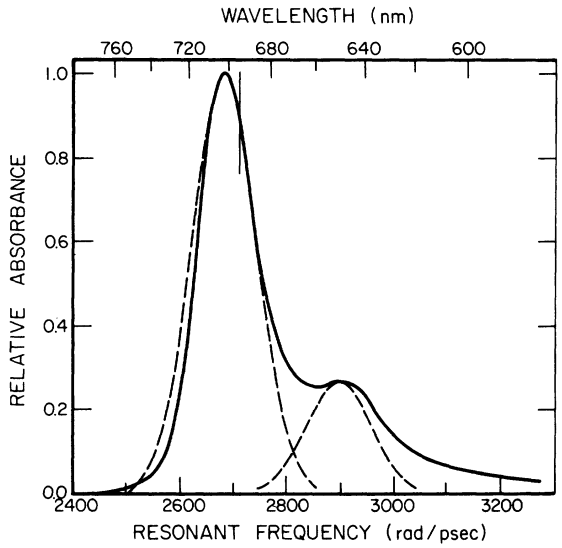


FIG. 3. Cryptocyanine-methanol absorption spectrum [after L. Huff, Ph.D. thesis (University of Southern California, 1969) (unpublished data)]. Gaussian substructure (dashed lines) shows the resolution of the spectrum into two vibrational peaks. A vertical line indicates the position of the ruby-laser wavelength.

assumption of homogeneous broadening, their theory shows steady-state transmission to be governed by the flux-density-dependent absorption coefficient

$$\alpha(F) \equiv -\frac{1}{F}\frac{dF}{dx} = N_0\sigma\frac{1+AF\sigma\tau}{1+BF\sigma\tau+A(F\sigma\tau)^2T_t'/\tau}, \tag{47}$$

where $\tau = T_1T_c/(T_1+T_c)$, $A=\sigma' T_t/\sigma T_c$, and $B = 1+(T_t/T_c)$. The relaxation times $T_1$, $T_t$, $T_t'$, and $T_c$ are associated with singlet-singlet decay, triplet-singlet decay, triplet-triplet decay, and intersystem crossing, respectively. The curve drawn through the data of Fig. 1 is obtained by integrating Eq. (47) when $\sigma = 7.2\times10^{-16}$ cm$^2$, $\sigma'/\sigma = 0.36$, $\tau = 40$ psec, $T_t/T_c = 2.0$, and $T_t' = 0.04$ psec. When these values are employed in the equation, the condition $\alpha(F) = \frac{1}{2}\alpha(0)$ is satisfied at the intensity $6.41\times10^6$ W/cm$^2$. This may be regarded as a characteristic intensity for Beer's-law violation consistent with the Huff-DeShazer (HDS) model and data.

### 2. *Analysis based on inhomogeneous broadening*

While the use of Eq. (47) gives a satisfactory fit to experiment at low intensities, it does not account for the transmission decrease that Huff and DeShazer observe above $10^8$ W/cm$^2$. More importantly, the model assumes an homogeneously broadened absorber inconsistent with observations of hole burning in cryptocyanine-methanol.[5,6] These difficulties are circumvented through use of the molecular model we have developed in Secs. II and III. Equation (31) for the absorption coefficient shows that wave transmission depends on six molecular parameters: $\sigma$, $\sigma'$, $\sigma_h$, $T_1$, $T_2$, and $T_3$. Of these, $\sigma$ and the ratio $\sigma_h/T_2$ may be determined from a sample's absorption spectrum. In Fig. 3 we have resolved the cryptocyanine-methanol spectrum into two peaks, according to Eq. (45). The inhomogeneous distribution $g(\omega_0-\bar{\omega}_0)$ is taken to be a Gaussian function of standard deviation $\frac{1}{2}\Delta\omega = 60$ psec$^{-1}$. With $\sigma = 7.2\times10^{-16}$ cm$^2$ at 694.3 nm, we are led to $\sigma_h/T_2 = 4.14\times10^{-14}$ cm$^2$/psec. In order to apply the steady-state results of Sec. III, it is necessary to neglect transitions to the secondary peak in the cryptocyanine spectrum. The absorption coefficient of Eq. (31) is then specified when the four parameters $\sigma'$, $T_1$, $T_2$, and $T_3$ are given.

We hope to obtain information about these parameters from the data of Fig. 1. Transmission curves analogous to the one of Huff and DeShazer may be obtained from Eq. (32). The choice of molecular parameters to give a good fit to the data may be based on the following characteristics: (i) significant Beer's-law violation begins in the range $10^6$–$10^7$ W/cm$^2$; (ii) a transmission maximum occurs at ~$10^8$ W/cm$^2$; (iii) the transmission value at this maximum is 70%. These features may be described more precisely (if somewhat arbitrarily) in terms of conditions placed on the absorption co-

efficient: (a) $\alpha(F)=\frac{1}{2}\alpha(0)$ at the intensity $I=\hbar\omega F=6.41\times10^6$ W/cm$^2$; (b) $d\alpha/dF=0$ at $I=10^8$ W/cm$^2$; (c) $\alpha=\alpha_{min}=\alpha(0)[(\ln70\%)/(\ln20\%)]=0.222\alpha(0)$ at $I=10^8$ W/cm$^2$.

Figure 4 illustrates how these criteria can be used to arrive at approximate values for $\sigma'$, $T_1$, $T_2$, and $T_3$. Curves designated A in Fig. 4 show the value $T_3$ must have to satisfy condition (a) when $\sigma'$, $T_1$, and $T_2$ are given. The physical requirement $T_3 \geq T_2$ accounts for an upper limit on the dephasing time. Curves labeled B indicate the intensity at which $d\alpha/dF=0$ for $\sigma'$, $T_1$, and $T_2$ given, and $T_3$ chosen from A. The remaining curves, C, show the value of $\alpha_{min}/\alpha(0)$ corresponding to this intensity.

Conditions (a), (b), and (c) appear to be best satisfied for $T_1\cong10$ psec, $T_2\cong0.4$ psec, and $T_3\cong10$ psec. The ratio $\sigma'/\sigma=0.36$ has been used in the construction of Fig. 4. Additionally, we have examined parameter behavior for $\sigma'/\sigma=0.12$, 0.24, and 0.48, and we have chosen 14 values for $\sigma'$, $T_1$, $T_2$, and $T_3$ that appear to be most consistent with experimental transmission data.

These selections are listed in Table I. The order of appearance roughly indicates the success of a given parameter set in providing a fit to Fig. 1, using Eq. (32). All choices exactly satisfy $\alpha(F)=\frac{1}{2}\alpha(0)$ at $6.41\times10^6$ W/cm$^2$, and this leads to close agreement with the HDS theoretical curve at low intensities. In fact, all 14 choices yield transmission curves within 1% of the HDS result at light levels below $10^7$ W/cm$^2$. The deviation at higher intensities may be seen in Fig. 5 for parameter sets 1, 7, and 13 of Table I.

TABLE I. Sets of values for $\sigma'$, $T_1$, $T_2$, and $T_3$ consistent with the experimental data of Fig. 1.

| Set no. | $\sigma'$ ($10^{-16}$ cm$^2$) | $T_1$(psec) | $T_2$(psec) | $T_3$(psec) |
|---|---|---|---|---|
| 1 | 3.456 | 10 | 0.9250 | 2.673 |
| 2 | 2.592 | 10 | 0.4582 | 7.208 |
| 3 | 3.456 | 10 | 1.266 | 1.266 |
| 4 | 3.456 | 10 | 0.6975 | 4.257 |
| 5 | 2.592 | 10 | 0.5689 | 5.361 |
| 6 | 2.592 | 25 | 1.175 | 1.175 |
| 7 | 2.592 | 25 | 0.8587 | 2.481 |
| 8 | 1.728 | 50 | 0.4178 | 3.916 |
| 9 | 1.728 | 25 | 0.4066 | 6.378 |
| 10 | 2.592 | 10 | 0.9010 | 2.604 |
| 11 | 1.728 | 75 | 0.5667 | 1.155 |
| 12 | 1.728 | 100 | 0.1352 | 3.746 |
| 13 | 1.728 | 50 | 0.8986 | 0.8986 |
| 14 | 0.864 | 50 | 0.092 | 25.0 |

The analysis employed here is subjective to some degree, and we would hesitate to propose any values for $\sigma'$, $T_1$, $T_2$, and $T_3$ as being more likely than any other values that provide a reasonable fit to experiment. However, the results do show the feasibility of explaining the data of Huff and DeShazer using a simple molecular model requiring no relaxation time longer than about 10 psec. The unimportance of the triplet state in this model is consistent with the demonstrated usefulness of cryptocyanine as a mode-locking agent for the ruby laser,[23] and as a dye-laser material in its own right.[24] Moreover, the assumed inhomogeneity of

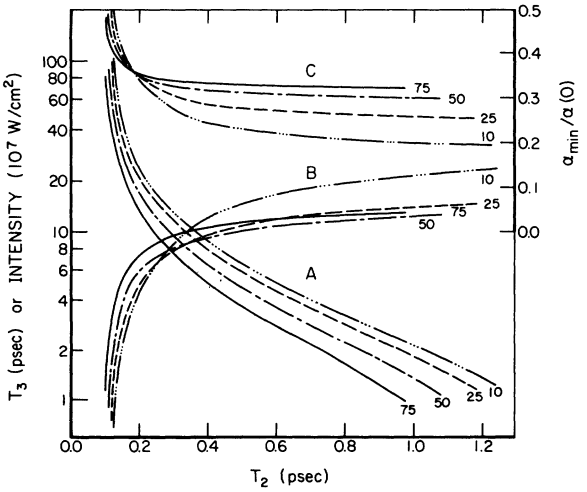


FIG. 4. Curves: (A), $T_3$-vs-$T_2$ behavior determined by criterion (a) of the text. (B), $T_2$ variation of the intensity at which $d\alpha/dF=0$, given $T_3$ chosen from curves A. (C), (Right vertical axis), corresponding $T_2$ variation of $\alpha_{min}/\alpha(0)$. Numbers associated with each curve designate $T_1$ (psec). $\sigma'=\sigma\times0.36$ throughout.

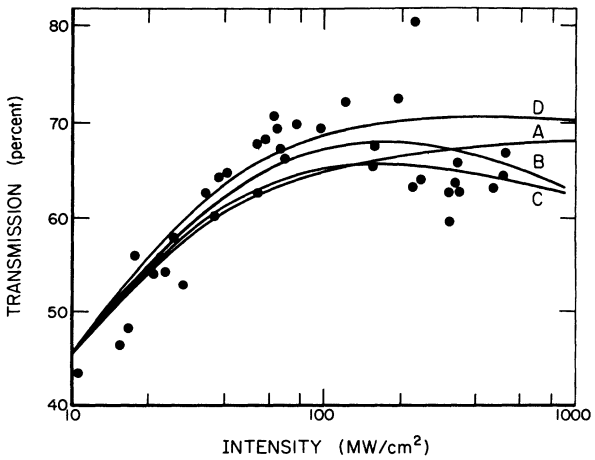


FIG. 5. Transmission-vs-intensity behavior of cryptocyanine-methanol above 10 MW/cm$^2$. Data points and curve A are taken from Fig. 1. Curves B, C, and D are, respectively, associated with parameter sets 1, 7, and 13 of Table I.

absorption in the model we have employed is automatically consistent with the evidence of hole burning in cryptocyanine.[5,6]

### B. Ultrashort-pulse transmission in DDI-glycerin

A steady-state transmission experiment of the type just described gives some information about a number of molecular parameters, but no precise information about any one. An opposite situation applies when transmission experiments are performed with pulses short in comparison to $T_1$ and $T_3$, but long in comparison to $T_2$. Then one sacrifices information about $T_1$ and $T_3$ to gain fairly precise information about $T_2$. This will be demonstrated using the short-pulse results of Sec. III.

Figure 6 shows an experiment which we have used to determine a collisional dephasing time of $0.4 \pm 0.2$ psec for DDI molecules in glycerin. A train of ~100-psec pulses from a mode-locked ruby laser is incident on a 1-cm sample of the dye. The pulse energy directed into the sample is proportional to the signal designated $E$ in Fig. 6(b), while the output energy is represented by signal $\mathcal{O}$. A glass flat reflects about 4% of the output beam through the sample a second time, and the light transmitted in this passage is signal $P$. The three pulses $P$, $\mathcal{O}$, and $E$ are eventually collected at the cathode of a United Aircraft model 1240 phototransducer. Their time of arrival is staggered at ~4-nsec intervals so that each may be resolved on the screen of a Tektronix 519 oscilloscope, and so that the measurement may be repeated for all excitation pulses emitted by the laser, 13 nsec apart. The ratios $P/\mathcal{O}$ and $\mathcal{O}/E$ indicate the energy transmission of probe and exciting pulses, respectively.

The first experimental results to be described are shown in Fig. 7. Data points in the lower range

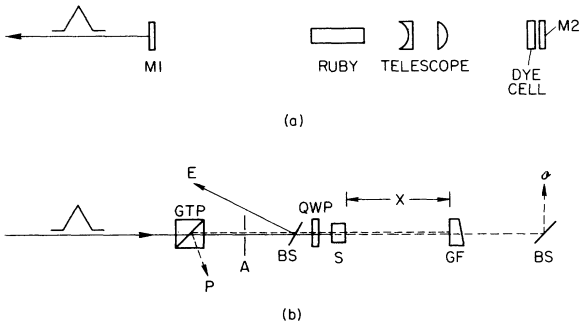


FIG. 6. Experimental arrangement for short-pulse transmission measurements. (a) Laser configuration: $M1, M2$ = dielectric mirrors. (b) Optics and sample configuration: A = aperture; BS = beam splitter; GF = glass flat; GTP = Glan-Thompson polarizer; QWP = quarter-wave plate; S = sample; $2X/c$ = probe delay time.

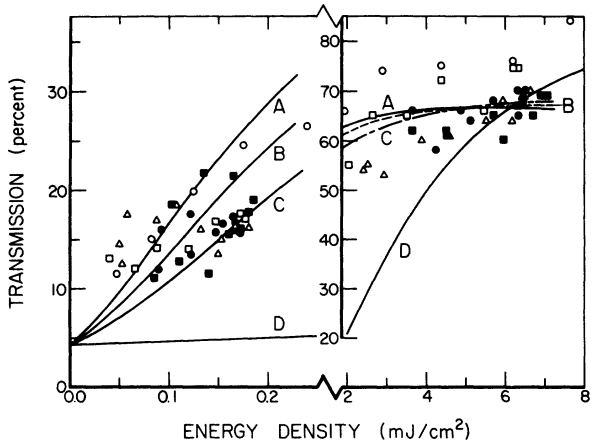


FIG. 7. Transmission vs incident energy density for DDI-glycerin. Symbols ○, △, □, ●, and ■ designate pulses from five different trains employed in the experiment. Theoretical curves: (A) $T_2 = 0.5$ psec, $\sigma' = 1.1 \times 10^{-16}$ cm$^2$; (B) $T_2 = 0.4$ psec, $\sigma' = 0.88 \times 10^{-16}$ cm$^2$; (C) $T_2 = 0.3$ psec, $\sigma' = 0.66 \times 10^{-16}$ cm$^2$; (D) homogeneously broadened limit ($T_2 \to 0$).

of input energies are associated with probe transmissions at delays of 1.7–2.0 nsec following excitation. Closed symbols are used to describe experiments in which the probe beam was slightly misaligned to permit sampling of an unexcited dye region. Since transmission was not sensitive to this adjustment, we conclude that recovery of ground-state absorption was essentially complete at the delays examined.

The higher range of input energies in Fig. 7 is associated with excitation pulses. Compared to the situation found to exist in the probe regime, transmission is relatively insensitive to variations in pulse energy. The suggestion is that all excitation pulses are energetic enough to pump a large fraction of dye molecules into a slightly absorbing excited state.[25]

We can account for the observed behavior of DDI-glycerin through use of the energy attenuation Eq. (38). In view of the double-peaked structure of the DDI-glycerin absorption spectrum, as seen in Fig. 8, it is necessary to modify Eq. (37b) for $f(W)$ by incorporating the transformation of Eq. (44). Then short-pulse transmission is specified in terms of the molecular parameters $\sigma_h$, $\sigma'$, $k_1^2$, $\Delta_1$, and $\bar{\omega}_0$. Since the last three quantities and the ratio $\sigma_h/T_2$ may be obtained from a sample's absorption spectrum, a theoretical fit to the data of Fig. 7 depends only on the choice of cross section $\sigma'$ and dephasing time $T_2$.

We have resolved the DDI-glycerin spectrum into two Gaussian peaks of standard deviation $\frac{1}{2}\Delta\omega = 75$ psec$^{-1}$. The separation of the peaks is $\Delta_1 = 230$

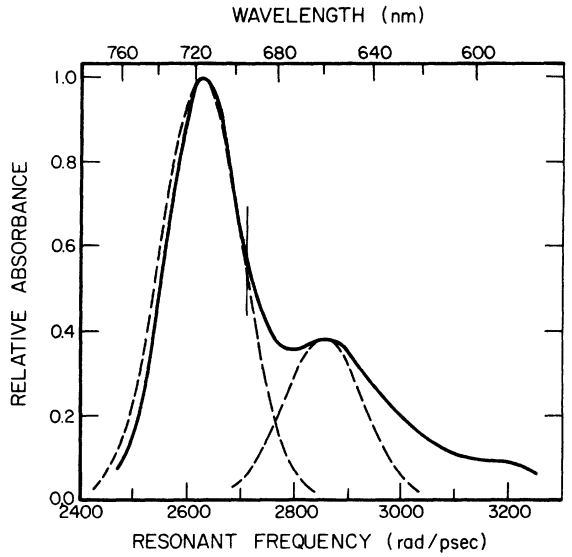


FIG. 8. DDI-glycerin absorption spectrum. Gaussian substructure (dashed lines) shows the resolution of the spectrum into two vibrational peaks. A vertical line indicates the position of the ruby-laser wavelength.

psec$^{-1}$ and the relative strength of the secondary peak is $k_1^2 = 0.38$. The center frequency of the main transition is $\bar{\omega}_0 = 2627$ psec$^{-1}$, corresponding to $\bar{\lambda}_0 = 717$ nm. The ratio $\sigma_h/T_2 = 4.57\times10^{-14}$ cm$^2$/psec is consistent with $\sigma = 4.4\times10^{-16}$ cm$^2$ at the ruby-laser wavelength.[26]

We have used these results in Eq. (38) to compute the energy variation of $W(1\text{ cm}, \infty)/W(0, \infty)$ for several values of $\sigma'$ and $T_2$. The absorber concentration $N_0$ is chosen to give a minimum sample transmission of 4.3%, consistent with experiment. The transmission-vs-energy curves so obtained are designated A, B, and C in Fig. 7. The analysis indicates a dephasing time of $0.4 \pm 0.2$ psec for DDI-glycerin.

In addition to the wide scattering of data points, principal sources of uncertainty are (i) the energy calibration of the horizontal axis of Fig. 7, and (ii) the use of an estimated value for $\sigma$.[26] Moreover, we have neglected throughout the anisotropic nature of DDI. On the basis of the conjugated-chain structure of this polymethine dye, it should absorb as a linear oscillator.[27] In particular, it should absorb linearly and circularly polarized light in different amounts, as described by Eq. (43).

Consider again the experimental configuration of Fig. 6(b). The quarter-wave plate is so positioned with respect to the sample that both exciting and probe pulses are circularly polarized. Data obtained in this way is that which has been plotted in Fig. 7. We have also studied the transmission of linearly polarized light using a modified configuration in which a shift of the quarter-wave plate to the opposite side of the sample was the major change. If the theoretical ideas culminating in Eq. (43) are correct, we expect to observe a difference in transmission as a function of optical polarization.

The data for this experiment are shown in Fig. 9. The circles (squares) show the transmission variation of circularly (linearly) polarized light. In contrast to Fig. 7, each datum does not represent the transmission and incident energy of a single pulse, but rather the average transmission and average energy of all pulses located within a particular increment of 0.025 mJ/cm$^2$ incident energy. The error bars are statistically determined. They reflect experimental uncertainties for individual pulses reduced by the square root of the number of pulses averaged to obtain a given datum. Typically, this number was two in the case of linear polarization and six in the case of circular polarization.

The theoretical curves presented in Fig. 9 are obtained from solutions of the energy-attenuation

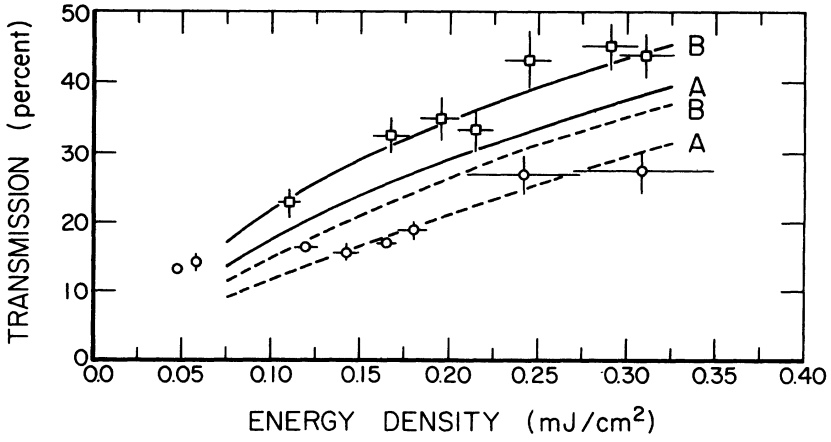


FIG. 9. Polarization dependence of absorption by DDI-glycerin. Symbols ○ and □ designate circularly and linearly polarized light, respectively. Theoretical transmission-vs-energy density behavior is plotted for $T_2 = 0.3$ psec (curves A), $T_2 = 0.4$ psec (curves B), circular polarization (dashed curves), and linear polarization (solid curves).

equation (43). We have accounted for the existence of two excited vibronic transitions in DDI-glycerin, consistent with its absorption spectrum. However, we have neglected excited-state absorption now since we are concerned with pumping energies too low to significantly populate the upper level and since the ratio $\sigma'/\sigma \cong 0.20$ is rather small anyway.

The theoretical fit to the data is not perfect for either $T_2 = 0.3$ or 0.4 psec, but we are encouraged that the theory accounts for the major features of the polarization dependence of absorption. One possible source of discrepancy was a slight deterioration of the sample that occurred prior to taking the linearly polarized data of Fig. 9. (The low-intensity sample transmission at 694 nm went from ~4.3% to ~5.1%.) Also note that we have assumed DDI to be a strictly linear oscillator and that we have neglected all molecular reorientation over the 100-psec time span of the pulse. The success of the theory is to some degree a vindication of these assumptions. Our confidence in the assignment $T_2 = 0.4 \pm 0.2$ psec is increased by the results shown in Fig. 9.

## V. DISCUSSION AND CONCLUSIONS

While the development of picosecond spectroscopy has done much to increase our understanding of short-lived molecular phenomena, collisional dephasing and spectral cross relaxation are two important processes that have not been given a great deal of attention, either from an experimental or theoretical point of view. We have presented a semiclassical theory that accounts for the influence of $T_2$ and $T_3$ processes on the attenuation of intense laser light by inhomogeneously broadened organic-dye solutions. We have used our results to analyze several transmission experiments for the information they contain about the rates of spectral cross relaxation and collisional dephasing in liquids.

To our knowledge, the determination that $T_2 = 0.4 \pm 0.2$ psec in DDI-glycerin is the first that has been made for a solute organic dye. The value is consistent with the fact that photon echoes and self-induced transparency have not been observed in liquid systems. To do so in DDI-glycerin, at least, would require pulses an order of magnitude shorter than those presently available.

A natural extension of the work described here would be to measure $T_1$, $T_2$, and $\sigma'$ using ultrashort-pulse techniques, and then to employ the experiment of Huff and DeShazer[9] to obtain $T_3$ with fair precision. In the absence of short-pulse data for the system cryptocyanine-methanol, the analysis of Sec. IV leads us to suggest

$$0.1 \lesssim T_2 \lesssim 1.0 \text{ psec}, \quad 10 \gtrsim T_3 \gtrsim 1.0 \text{ psec}.$$

We would comment on the physical reasonableness of these results. Consider a methanol molecule with $kT$ of translational energy moving toward a solute dye 3 Å away. At room temperature the distance would be covered in 5 psec. This indicates a mean collision time of roughly 10 psec per molecule. If cryptocyanine is solvated by 17 methanol molecules, as Mourou *et al.* suggest,[28] then a value for $T_2$ in the range 0.1–1.0 psec is quite understandable.

Unfortunately, it is not possible to extend this argument to provide an estimate of $T_3$. Nor have there been any direct measurements of this time with which to compare our results. However, Mourou *et al.*[16] have suggested that the solvent reordering associated with the excitation of a polarizable dye molecule requires 10 psec in cryptocyanine. Also, the vibrational deactivation of excited molecules in liquids is typically found to take from 1 to 10 psec.[14,15,29] These results are the best indications available that the limits we have proposed for $T_3$ are physically reasonable ones.

Of necessity, our determinations of collision and cross-relaxation times have been indirect and therefore model dependent. Our confidence in the model is established by the facility with which it accounts for experimental transmission behavior. If future research enforces this confidence, the theory implemented in this paper will provide a valuable new tool for the study of subtle molecular interactions on a picosecond and subpicosecond time scale.

## ACKNOWLEDGMENTS

This work, particularly in its experimental aspects, was supported by the U.S. Air Force Office of Scientific Research. Much of the theory and data analysis were made possible through fellowship support by Battelle Memorial Institute, for which one of us (D.V.) is very grateful. That author also wishes to thank Dr. C. W. Kern for his encouragement and interest in this work throughout its final stages.

[1]N. Bloembergen, E. M. Purcell, and R. V. Pound, Phys. Rev. 73, 679 (1948).
[2]E. L. Hahn, Phys. Rev. 80, 580 (1950).
[3]G. E. Pake, *Paramagnetic Resonance* (Benjamin, New York, 1962), Chap. 5, p. 108.
[4]M. Hercher, Appl. Opt. 6, 947 (1967).
[5]M. L. Spaeth and W. R. Sooy, J. Chem. Phys. 48, 2315 (1968).
[6]G. Mourou, B. Drouin, and M. M. Denariez-Roberge, Opt. Commun. 8, 56 (1973).
[7]R. Wilbrandt, E. Mathieu, and H. Weber, Opt. Commun. 3, 328 (1971).
[8]J. D. Macomber, J. Appl. Phys. 38, 3525 (1967).
[9]L. Huff and L. G. DeShazer, J. Opt. Soc. Am. 60, 157 (1970).
[10]M. Andorn and K. H. Bar-Eli, J. Chem. Phys. 55, 5008 (1971); H. Schüller and H. Puell, Opt. Commun. 3, 352 (1971); C. R. Guiliano and L. D. Hess, IEEE J. Quantum Electron. QE-3, 358 (1967).
[11]S. L. McCall and E. L. Hahn, Phys. Rev. 183, 457 (1969).
[12]I. D. Abella, N. A. Kurnit, and S. R. Hartmann, Phys. Rev. 141, 391 (1966).
[13]B. B. Snavely, Proc. IEEE 57, 1374 (1969).
[14]P. M. Rentzepis, M. R. Topp, R. P. Jones, and J. Jortner, Phys. Rev. Lett. 25, 1742 (1970).
[15]P. M. Rentzepis, Chem. Phys. Lett. 2, 117 (1968).
[16]In this case states $|c\rangle$ and $|a\rangle$ are identical, but the energy gap between $|a\rangle$ and $|b\rangle$ is decreased by the solvent reordering. See G. Mourou, B. Drouin, M. Bergeron, and M. M. Denariez-Roberge, IEEE J. Quantum Electron. QE-9, 745 (1973); W. S. Struve, P. M. Rentzepis, and J. Jortner, J. Chem. Phys. 59, 5014 (1973); and also M. M. Malley and G. Mourou, Opt. Commun. 10, 323 (1974).
[17]R. Karplus and J. Schwinger, Phys. Rev. 73, 1020 (1948).
[18]W. E. Lamb, Jr., Phys. Rev. 134, A1429 (1964).
[19]G. L. Lamb, Jr., Rev. Mod. Phys. 43, 99 (1971).
[20]P. Kafalas, J. I. Masters, and E. M. E. Murray, J. Appl. Phys. 35, 2349 (1964).
[21]M. Hercher, W. Chu, and D. L. Stockman, IEEE J. Quantum Electron. QE-4, 954 (1968); B. H. Soffer and B. B. McFarland, Appl. Phys. Lett. 8, 166 (1966).
[22]R. I. Scarlet, J. F. Figueira, and H. Mahr, Appl. Phys. Lett. 13, 71 (1968); M. M. Malley and P. M. Rentzepis, Chem. Phys. Lett. 3, 534 (1969); G. Mourou, B. Drouin, M. Bergeron, and M. M. Denariez-Roberge, IEEE J. Quantum Electron. QE-9, 745 (1973); E. G. Arthurs, D. J. Bradley, and A. G. Roddie, Opt. Commun. 8, 118 (1973).
[23]M. E. Mack, IEEE J. Quantum Electron. QE-4, 1015 (1968).
[24]M. L. Spaeth and D. P. Bortfeld, Appl. Phys. Lett. 9, 179 (1966).
[25]Excited-state absorption in DDI-glycerin has been demonstrated by K. Razi Naqvi, D. K. Sharma, and G. J. Hoytink, Chem. Phys. Lett. 22, 5 (1973). However, their reported value $T_1 \approx 110$ psec is in conflict with our observation that ground-state recovery requires about 700 psec in DDI-glycerin. We employed a probe-delay technique similar to that of Scarlet *et al.* (Ref. 22). The experimental configuration was essentially that of Fig. 6.
[26]Because DDI molecules are not readily soluble in glycerin, the cross section $\sigma$ is difficult to measure in the conventional way. The value $\sigma = 4.4 \times 10^{-16}$ cm$^2$ is an estimate based on the DDI-methanol spectrum of N. I. Fisher and F. M. Hammer, Proc. R. Soc. Lond. A154, 703 (1936). An assumption is made that DDI has the same $f$ number in both glycerin and methanol.
[27]H. Kuhn, J. Chem. Phys. 17, 1198 (1949).
[28]G. Mourou, G. Busca, and M. M. Denariez-Roberge, Opt. Commun. 4, 40 (1971).
[29]A. Laubereau, D. von der Linde, and W. Kaiser, Phys. Rev. Lett. 28, 1162 (1972).